Electronic supplementary information (ESI) for New Journal of Chemistry.

Pd/meso-CoO derived from in situ reduction of the one-step synthesized Pd/meso-Co_3O_4: High-performance catalysts for benzene combustion

Xingtian Zhao[a], Ran Zhang[b], Yuxi Liu[a], Jiguang Deng[a], Peng Xu[a,c], Sijie Lv[a], Shuang Li[a], Wenbo Pei[a], Kunfeng Zhang[a] and Hongxing Dai*[a]

[a] *Beijing Key Laboratory for Green Catalysis and Separation, Key Laboratory of Beijing on Regional Air Pollution Control, Key Laboratory of Advanced Functional Materials, Education Ministry of China, Laboratory of Catalysis Chemistry and Nanoscience, Department of Chemistry and Chemical Engineering, College of Environmental and Energy Engineering, Beijing University of Technology, Beijing 100124, China. E-mail: hxdai@bjut.edu.cn*

[b] *Petrochina Petrochemical Research Institute, Beijing 102206, China.*

[c] *CAS Key Laboratory of Standardization and Measurement for Nanotechnology, National Center for Nanoscience and Technology, Beijing 100190, China.*

Content

Catalyst characterization procedures:

Elemental analyses of the noble metal loadings were performed using the inductively coupled plasma–atomic emission spectroscopic (ICP–AES) technique on a Thermo Electron IRIS Intrepid ER/S spectrometer. X-ray diffraction (XRD) patterns of the samples were recorded on a Bruker D8 Advance diffractometer using the Cu Kα radiation and nickel filter, with a scanning speed of 1 °/min in the 2θ range of 0.5–10° and a scanning speed of 8° min^{-1} in the 2θ range of 10–85°. Transmission electron microscopic (TEM) images of the samples were obtained using the JEOL-2010 equipment (operating at 200 kV). High-angle annular dark field–scanning transmission electron microscopic (HAADF–STEM) and energy-dispersive X-ray spectroscopic (EDX) techniques were used to acquire the HAADF–STEM and element mapping images of the typical samples on the equipment FEI G2 80–200/Chemi-STEM with a probe corrector. The TEM and HAADF–STEM/EDX analyses on the samples were carried out by dispersing the sample powders in ethanol and depositing them on a copper grid.

Surface area measurements were carried out on a Micromeritics ASAP 2020 instrument via N_2 adsorption at –196 °C. Before the measurement, each sample was degassed at 250 °C for 3 h. Surface areas and pore-size distributions of the samples were calculated by the Brunauer–Emmett–Teller (BET) and Barrett–Joyner–Halenda (BJH) methods, respectively. X-ray photoelectron spectroscopy (XPS) was used to measure the Co 2p, O 1s, Pd 3d, and C 1s binding energies (BEs) of the surface species on the samples using a Thermo Fisher Scientific ESCALAB 250 Xi spectrometer equipped with the Mg Kα X-ray source (hv = 1253.6 eV). The samples were degassed in the preparation chamber (10^{-5} Torr) for 0.5 h and then introduced into the analysis chamber (3×10^{-9} Torr) for XPS spectrum recording. All of the signals were referenced to the BE (284.6 eV) of C 1s for calibration. Raman spectra of the

samples were recorded with a visible (532 nm) laser excitation on a Horiba-Jobin Yvon Laboratory Ram-HR Raman spectrometer with a confocal microscope and a notch filter (Kaiser Super Notch). The scattered photons were directed into a single monochromator and focused onto a UV-sensitive liquid N_2-cooled CCD detector (Horiba-Jobin Yvon CCD-3000V) with a spectral resolution of 1 cm^{-1}.

Hydrogen temperature-programmed reduction (H_2-TPR) experiments were carried out on a chemical adsorption analyzer (Autochem II 2920, Micromeritics) equipped with a thermal conductivity detector (TCD). Before H_2-TPR experiment, ca. 30 mg of the sample was loaded to a quartz fixed-bed U-shaped microreactor. The sample was first pretreated in an air or He flow of 30 mL min^{-1} at 300 ^oC for 1 h and cooled to RT at the same atmosphere. H_2-TPR profile of each sample was recorded when the sample was heated at a ramp of 10 ^oC min^{-1} in a mixture of 10 vol% H_2/90 vol% Ar (30 mL min^{-1}) from RT to 800 ^oC. The alteration in H_2 concentration of the effluent was monitored online by a TCD. The reduction peak was calibrated against that of the complete reduction of a known standard powered CuO (Aldrich, 99.995 %). Oxygen temperature-programmed reduction (O_2-TPD) experiments were conducted on the apparatus same as that used in the H_2-TPR experiments, and the samples were preheated using the same experimental conditions. After cooling to RT, an O_2 flow of 20 mL min^{-1} was introduced into the U-shaped microreactor for 1 h. Then, the sample was purged in a He flow of 30 mL min^{-1} for 1 h. O_2-TPD profile of each sample was recorded when the sample was heated at a ramp of 10 ^oC min^{-1} in a He flow of 30 mL min^{-1} from RT to 900 ^oC. The desorption amounts of oxygen were calculated according to the amount of an oxygen pulse monitored by a TCD.

In situ diffuse reflectance Fourier transform infrared spectroscopic (DRIFTS) experiments were performed on a Bruker FT-IR spectrometer (TENSOR II) equipped with a liquid nitrogen-cooling mercury-cadmium-telluride (MCT) detector. 30 mg of the sample was

placed in a high-temperature IR cell with a ZnSe window (Pike Technologies), and heated in a N_2 flow of 20 mL min^{-1} at 300 ^oC for 30 min to remove the adsorbed water and CO_2. During the temperature-cooling process, the background was collected in N_2 at different temperatures. Finally, the temperature was cooled to 150 ^oC. Afterward, a 1000 ppm benzene (N_2 as balance) flow of 10 mL min^{-1} was passed through the samples at 150 ^oC. Subsequently, gaseous and physisorbed benzene was purged by flushing N_2 for 30 min, and the temperature was increased in N_2 or 20 vol% O_2 (N_2 as balance) to 300 ^oC. The DRIFTS spectra in the range of 650–4000 cm^{-1} (with 32 scans at a resolution of 4 cm^{-1}) of the samples were recorded at different time and temperatures. In the other experiments, a mixture of 1000 ppm benzene + 20 vol% O_2 + N_2 was introduced to the sample at 150 ^oC, and the temperature was increased in the same atmosphere to 300 ^oC.

Catalytic activity evaluation procedures:

Catalytic activities of the samples were evaluated in a continuous-flow fixed-bed quartz tubular microreactor (i.d. = 6.0 mm). A thermocouple was inserted inside the catalyst bed (0.5 g of the catalyst (40–60 mesh) diluted with 1.5 g of quartz sand (40–60 mesh)) to measure the reaction temperatures. Before activity measurement, the samples were pretreated in a N_2 flow of 20 mL min^{-1} at 250 ^oC for 30 min. The 1000-ppm benzene gas was produced by a N_2 flow bubbling through a saturator filled with liquid benzene at 6 ^oC. A gas mixture composed of 1000 ppm benzene + 20 vol% O_2 + N_2 (balance) was fed into the microreactor with a total flow rate of 33.3 mL min^{-1}, equivalent to a space velocity (SV) of ca. 40 000 mL $(g\ h)^{-1}$. In the case of H_2O addition, 3.0 and 5.0 vol% H_2O was introduced by passing a N_2 flow of 19.2 mL min^{-1} through a water saturator at 34 and 43 ^oC, respectively. In the case of CO_2 introduction, 5.0 vol% CO_2 was introduced from a 30 vol% CO_2 (N_2 as balance) cylinder. The activity data were collected after steady operation at a given temperature for 30 min. The

reactants and products were online analyzed using Shimadzu GC-14C equipped with a flame ionization detector (Stabilwax column, 30 m in length) and a TCD (Porapak-Q column, 5 m in length). Benzene conversion (X) was calculated according to the equation: $X = ([C_6H_6]_{in} - [C_6H_6]_{out})/[C_6H_6]_{in} \times 100\ \%$, where $[C_6H_6]_{in}$ and $[C_6H_6]_{out}$ were the inlet and outlet benzene concentrations, respectively. CO_2 yield (Y) was estimated according to the formula: $Y = ([CO_2]_{out}/([C_6H_6]_{in} \times 6)) \times 100\ \%$, where $[CO_2]_{out}$ was the effluent CO_2 concentration.

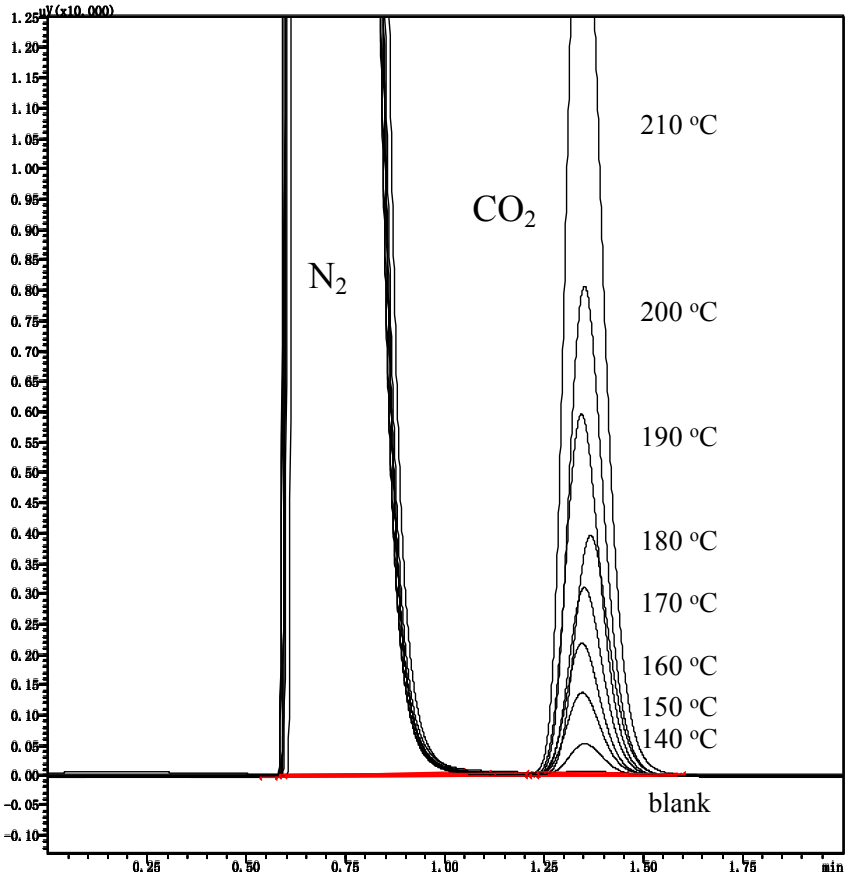

Fig. S1 GC spectra of CO_2 formed during the benzene oxidation processes over 0.85Pd/meso-Co_3O_4 at SV = 40 000 mL $(g\ h)^{-1}$.

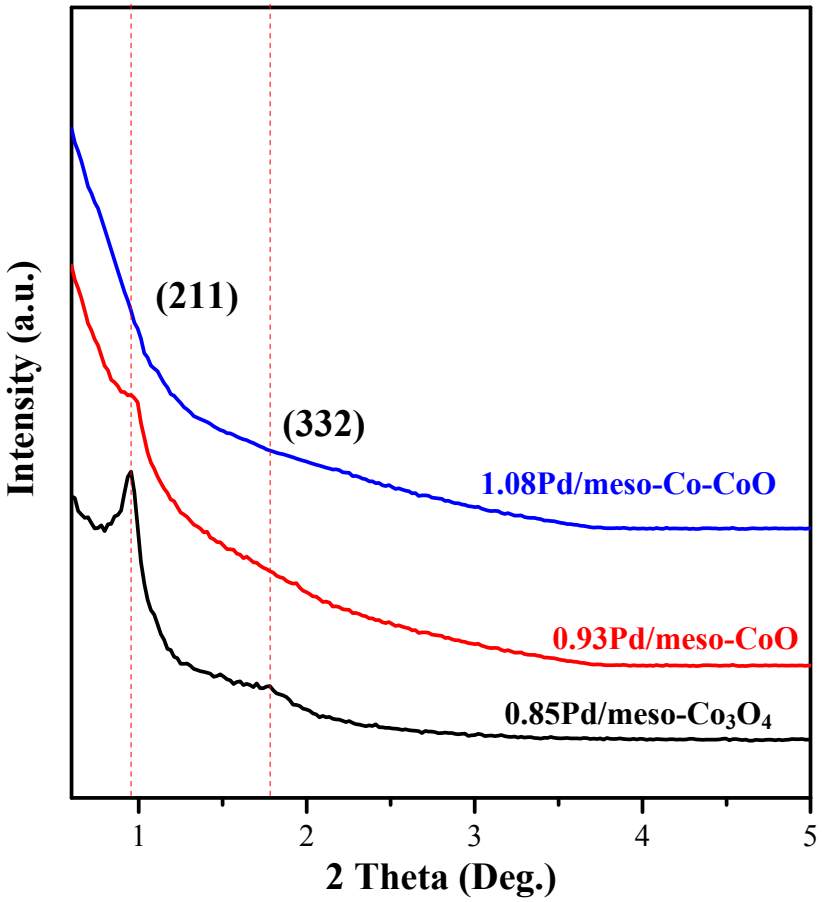

Fig. S2 Low-angle XRD patterns of the samples.

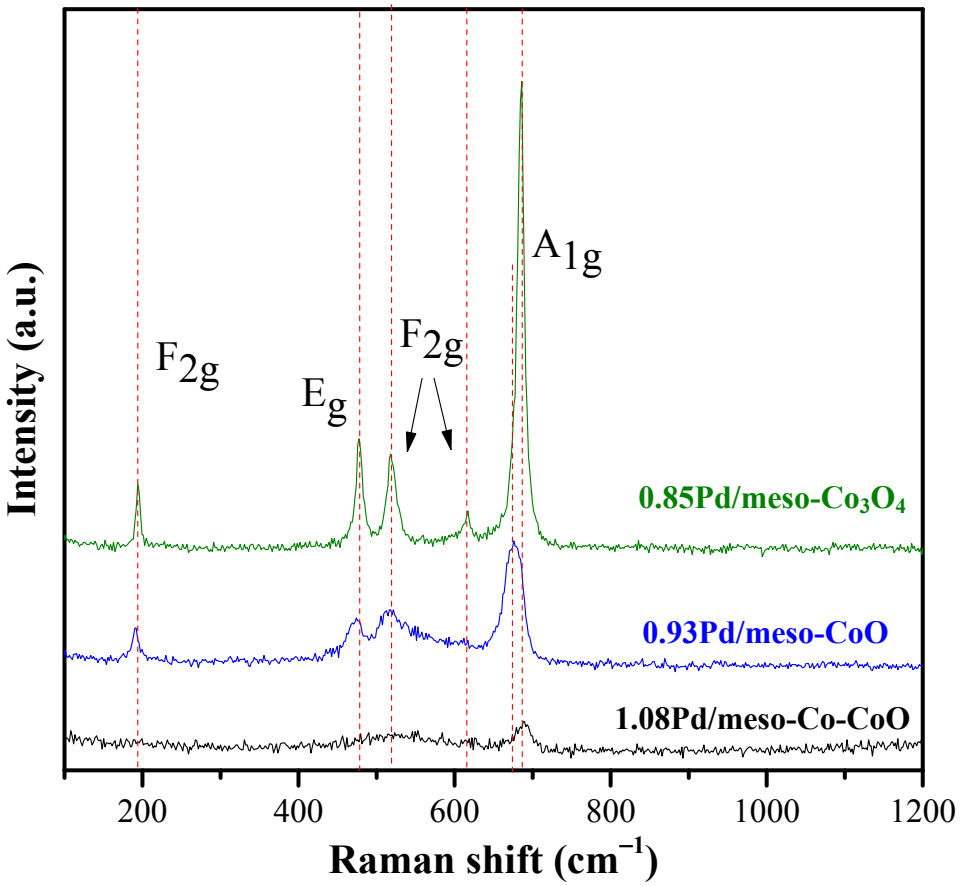

Fig. S3 Raman spectra of the samples.

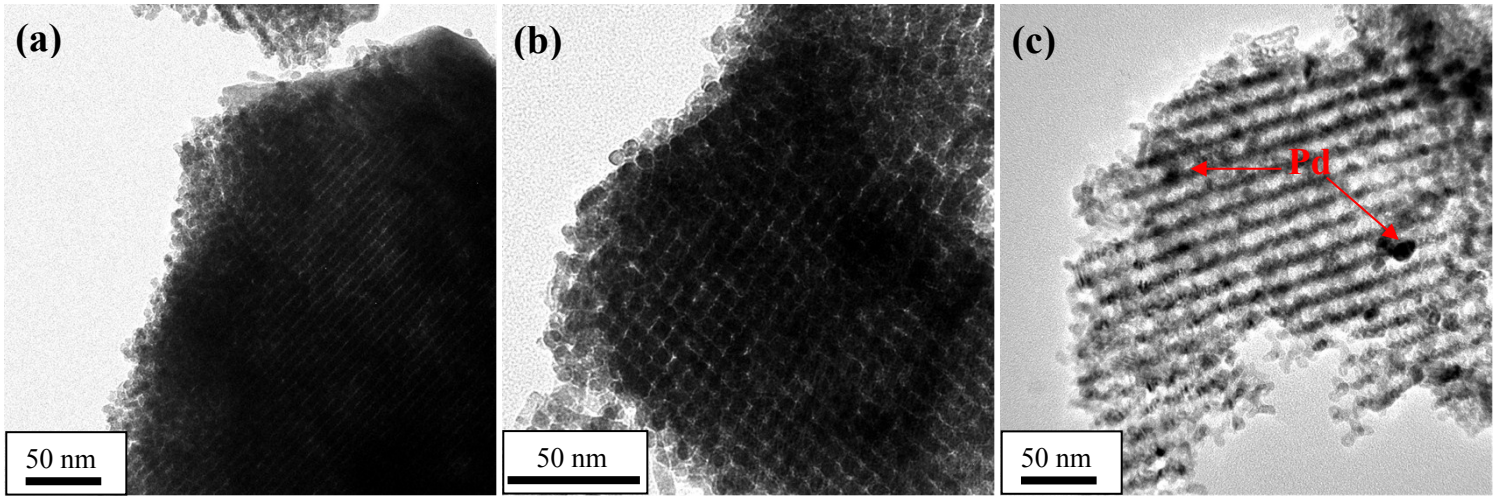

Fig. S4 TEM images of (a) 0.85Pd/meso-Co_3O_4, (b) 0.93Pd/meso-CoO, and (c) 1.08Pd/meso-Co-CoO.

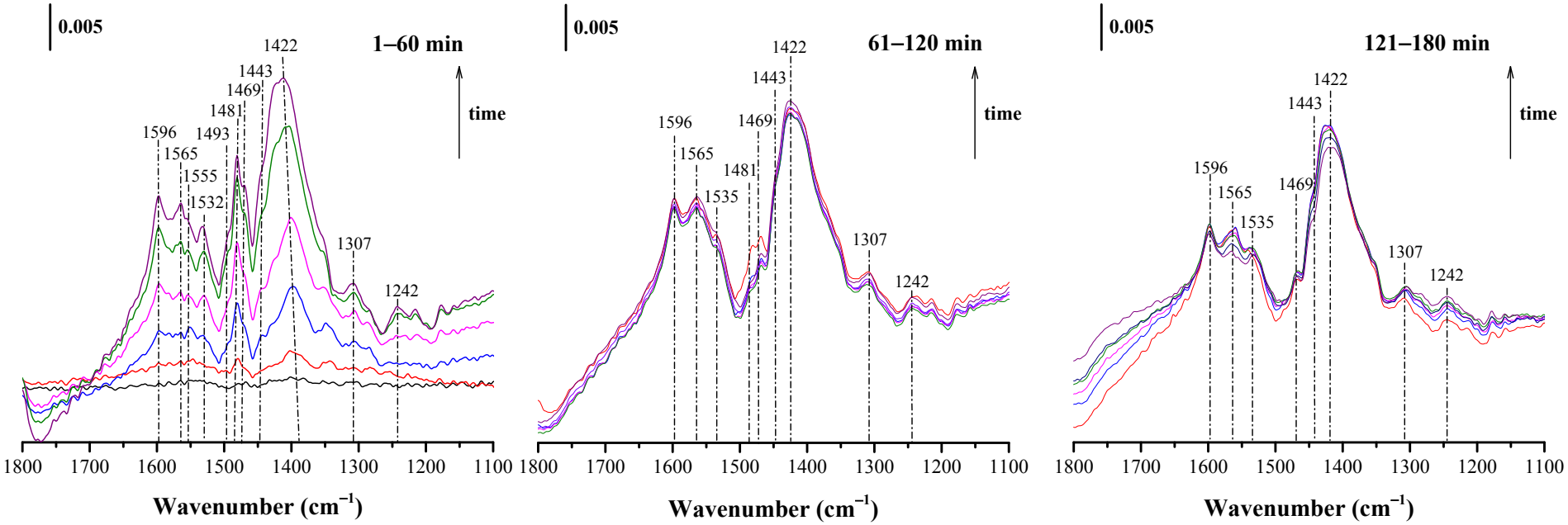

Fig. S5 *In situ* DRIFTS spectra of adsorbed intermediates on the 0.85Pd/meso-Co_3O_4 sample in the flow of 1000 ppm benzene + N_2 (in the range of 1–60 min), N_2 (in the range of 61–120 min), and 20 vol% O_2 + N_2 (in the range of 121–180 min) at 150 °C, respectively.

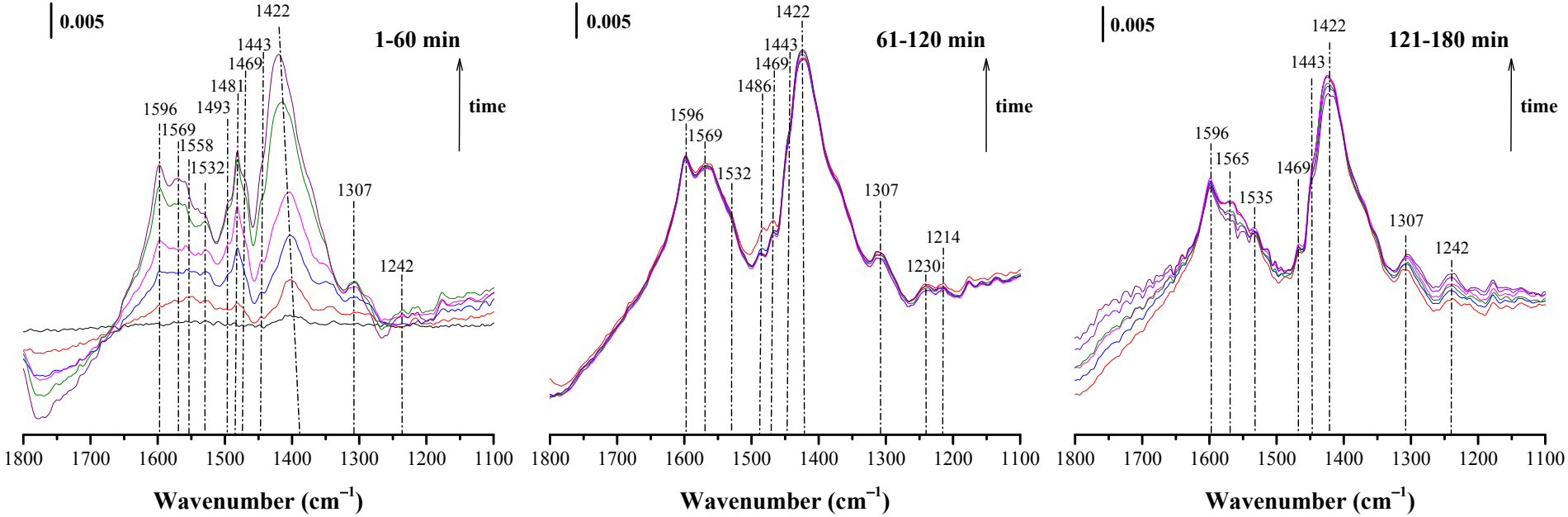

Fig. S6 *In situ* DRIFTS spectra of adsorbed intermediates on the 0.93Pd/meso-CoO sample in the flow of 1000 ppm benzene + N_2 (in the range of 1–60 min), N_2 (in the range of 61–120 min), and 20 vol% O_2 + N_2 (in the range of 121–180 min) at 150 °C, respectively.

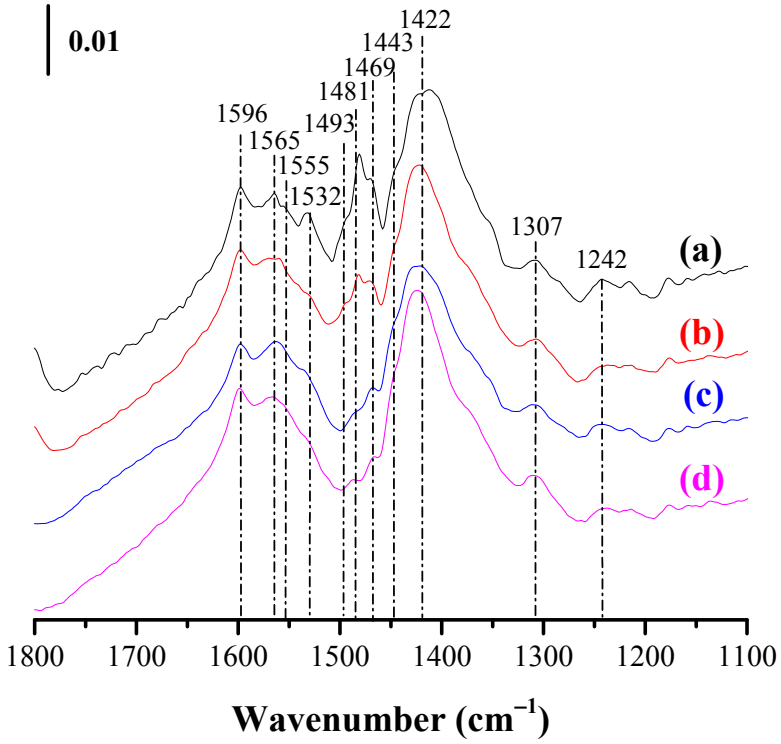

Fig. S7 *In situ* DRIFTS spectra of (a, c) 0.85Pd/meso-Co_3O_4 and (b, d) 0.93Pd/meso-CoO after adsorption of 1000 ppm benzene at 150 °C for 1 h and N_2 purging for 1 h.

Table S1 Catalytic activities for benzene oxidation over the catalysts reported in this work and the literature

Catalyst	Reaction condition	Space velocity (mL (g h)$^{-1}$)	$T_{90\%}$ (°C)	Benzene oxidation at 160 °C		Ref.
				$TOF_{noble\ metal}$ ($\times 10^{-3}$ s^{-1})	Specific reaction rate (μmol ($g_{noble\ metal}$ s)$^{-1}$)	
0.85Pd/meso-Co_3O_4	1000 ppm C_6H_6 + air (balance)	40,000	214	0.62	5.85	This work
0.93Pd/meso-CoO	1000 ppm C_6H_6 + air (balance)	40,000	189	1.46	13.74	This work
1.08Pd/meso-Co-CoO	1000 ppm C_6H_6 + air (balance)	40,000	275	0.07	0.62	This work
K/Ag-OMS-40	1500 ppm C_6H_6 + air (balance)	90,000	218	1.28	11.90	[5]
1.0Pd/Al_2O_3	1500 ppm C_6H_6 + air (balance)	90,000	206	2.72	24.37	[5]
Ru-5Co/TiO_2	500 ppm C_6H_6 + 20 vol% O_2 + Ar (balance)	60,000	215	0.03	0.34	[43]
6.5Au/meso-Co_3O_4	1000 ppm C_6H_6 + air (balance)	20,000	189	0.33	1.68	[31]
0.53Pd/Co_3O_4	100 ppm C_6H_6 + air (balance)	60,000	221	0.30	2.82	[32]

Table S2 Assignments of the DRIFTS bands of the samples

Wavenumber (cm^{-1})	Vibrational mode	Species	Ref.
3002–3129	Phenylic C–H vibration	Gaseous benzene	[13]
1700–2000	Overtones	Gaseous benzene	[13]
1596	C–O antisymmetric vibration	Formate	[40]
1555–1565	C–O antisymmetric vibration	Acetate	[12,41,42]
1532	Superposition of the maleate and acetate species	Maleate, acetate	[42–44]
1481–1493	Skeletal C–C vibration	Aromatic ring	[40,44,45]
1469	C–H deformation vibration	Aromatic ring	[40,44,45]
1443	Skeletal C–C vibration	Aromatic ring	[40,44,45]
1400–1422	C–O symmetric vibration	Acetate	[12,42]
1307	C–H deformation vibration	Maleate	[42–44]
1242	–	Phenolate	[42]
600–1100	Phenylic C–H vibration	Gaseous benzene	[13]